


## Article

# Investigation of Structural and Optical Properties of Some [1,4]Dithiine-porphyrazine Dyes

Ola A. Abu Ali <sup>1</sup>, Hamada H. Abdel-Razik <sup>2,\*</sup>, Matokah Abualnaja <sup>3</sup> and Eman Fayad <sup>4,\*</sup> 

<sup>1</sup> Department of Chemistry, College of Science, Taif University, P.O. Box 11099, Taif 21944, Saudi Arabia; o.abuali@tu.edu.sa

<sup>2</sup> Chemistry Department, College of Science, Damietta University, New Damietta 34517, Egypt

<sup>3</sup> Department of Chemistry, Faculty of Applied Science, Umm Al-Qura University, Makkah al-Mukarramah 21955, Saudi Arabia; mmabualnaja@uqu.edu.sa

<sup>4</sup> Department of Biotechnology, Faculty of Sciences, Taif University, P.O. Box 11099, Taif 21944, Saudi Arabia

\* Correspondence: hamada@du.edu.eg (H.H.A.-R.); e.esmail@tu.edu.sa (E.F.)

**Abstract:** 1,4-Bis(p-tolylamino)-6,7-dichloroanthraquinone **1** when reacted with di(sodiothio)-maleonitrile **2** afforded heterocyclic thianone compound, 5,12-dioxo-5,12-dihydroanthro[2,3-b][1,4]dithiine-2,3-dicarbonitrile **3**. Using lithium/pentanol and acetic acid, the dicarbonitrile product **3** was cyclotetramerized, yielding the matching tetra 5,12-dioxo-5,12-dihydroanthro[2,3-b][1,4]dithiine-porphyrazine dye compound (2H-Pz) **4a**. The dicarbonitrile molecule was a ring-shaped metallic product utilizing metallic salt and quinoline, yielding the corresponding tetra 5,12-dioxo-5,12-dihydroanthro[2,3-b][1,4]dithiine-porphyrazinato-metal II dyes (M-Pz), M = Zn, Co, or Ni **4b–d**. The produced compounds' elemental analysis investigation, Infrared, and nuclear magnetic resonance spectrum information accord with the structures attributed to them. The cyclotetramerization and complexation reactions are ensured by the molecular weight and metal load of the produced products. The inclusion of electron-donating groups resulted in a lower optical band gap of the produced dye sensitizers, with “push-pull” promotion of about 1.55 eV. The prepared substituted porphyrazines reveal high absorption in the UV–VIS region, which could be of potential value as a building block for novel electronic and optical materials as well as a sensor for technology. This is considered for improving solar cell absorption. The absorption bands of the synthesized porphyrazine dyes extend beyond 800 nm, so these dyes could be useful in various optoelectronic applications.

**Keywords:** 1,4-bis(p-tolylamino); 6,7-dichloroanthraquinone; thianone; cyclotetramerization



**Citation:** Ali, O.A.A.; Abdel-Razik, H.H.; Abualnaja, M.; Fayad, E. Investigation of Structural and Optical Properties of Some [1,4]Dithiine-porphyrazine Dyes. *Molecules* **2022**, *27*, 1651. <https://doi.org/10.3390/molecules27051651>

Academic Editor: Antonio Zuorro

Received: 26 January 2022

Accepted: 27 February 2022

Published: 2 March 2022

**Publisher's Note:** MDPI stays neutral with regard to jurisdictional claims in published maps and institutional affiliations.



**Copyright:** © 2022 by the authors. Licensee MDPI, Basel, Switzerland. This article is an open access article distributed under the terms and conditions of the Creative Commons Attribution (CC BY) license (<https://creativecommons.org/licenses/by/4.0/>).

## 1. Introduction

In the broadest sense, optical substances change or control electromagnetic radiation in the ultraviolet (UV), visible, or infrared (IR) spectrum areas. These dyes are made into optical elements including lenses, reflections, screens, prisms, polarizers, sensors, and stimulators. Atoms and their electrical structures in the material interact with electromagnetic radiation (photons) at the microscopic scale to establish macroscopic optical properties. The external electric and magnetic fields applied to the material determine these optical properties. Optical materials can be made out of a wide variety of organic or inorganic materials [1]. Tetra-(1,4-dithiin)porphyrazine is one of the phthalocyanine derivatives having two sulfur atoms at equivalent 1,4-positions of the phthalocyanine benzene units [2]. Zinc, aluminium, and other metal porphyrazine complexes have anticancer characteristics and are used in photodynamic treatment [3]. In a multi-step reaction sequence, novel tetra-(1,4-dithiin) metal-free (H<sub>2</sub>-Pz) and metallo-porphyrazines (M-Pz, M = Mg, Fe) carrying peripheral tetra propyl-bromine were synthesized from 2,3-dicyano-5-propyl-bromine-1,4-dithiin and disodiummaleonitrile [4]. It was discovered that a new catalyst, iron (II) tetra (1,4-dithiin)porphyrazine, can be used to oxygenate the

breakdown of organic contaminants in aqueous solutions [5]. The peripherally peralkynylated phthalocyanine or naphthalocyanine analogues, namely tetra pyrazinoporphyrazines and tetra-6,7-quinoxalinoporphyrazines, are generated via base-induced cyclotetramerization of aromatic dinitriles with magnesium butoxide in refluxing butanol [6]. Iron (II)-tetramethyl-tetra (1,4-dithiin)porphyrazine was synthesized, and its photocatalytic characteristics were investigated [7]. The synthesis of metal-free and magnesium tetra-ester tetra(1,4-dithiin)porphyrazine was accomplished [8].

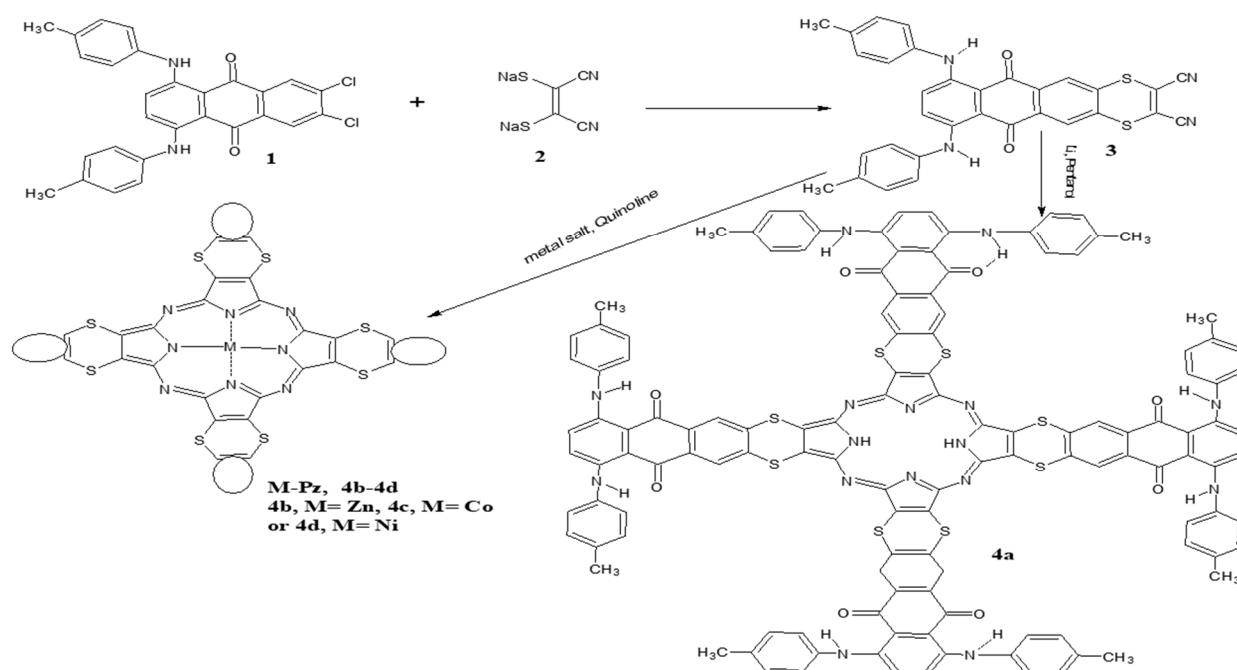
Zinc-tetra (1,4-dithiin)porphyrazine containing peripheral tetra propyl-bromine was synthesized, and its photocatalytic capabilities were described [9]. The photo-catalytic activity of peripheral substituents of cobalt thioporphyrazines has been described [10,11]. The photophysical and electrochemical properties of two porphyrin-chromophores have been explored [12]. The photophysical characteristics of three carbazole-fused zinc metallic porphyrin sensitizers were examined [13]. Porphyrazines are made by cyclizing maleonitrile with a magnesium template. Starting with the appropriate unsaturated dicarbonitrile derivative, metallic-porphyrazines were produced [14]. Compounds with more electrons and with low electron portions joined by a linkage have successfully been applied as rising alternatives [15–17].

The “push–pull” architecture of these “donor–acceptor” molecules facilitates the isolation of holes and electrons, reducing recombination. By cyclotetramerizing 1,2-bis(4-tert-butylphenylthio)maleonitrile in the presence of magnesium butanolate, magnesium porphyrazinate with eight 4-tert-butylphenylthio-groups on the peripheral locations has been produced [18,19]. Tetra(1,2,5-thiadiazolo)porphyrazine complexes with yttrium(III) and lutetium(III) were prepared, spectrally analyzed, and studied using DFT [20,21]. The electronic and geometric structures of porphyrazine (Pz) and tetrakis(1,2,5-thiadiazole)porphyrazine (TTDPz) metal complexes were studied [22]. There have been reports of organic/metal photosensitizers for dye-sensitized solar cells [23]. In this study, we aimed to create new porphyrazines that could be used as a key component for new electronic and optical compounds, as well as a technology sensor.

## 2. Results and Discussion

1,4-Bis(p-tolylamino)-6,7-dichloroanthraquinone **1** when condensed with di(sodiothio) maleonitrile **2** yielded di-carbonitrile derivative **3**. Using lithium/pentanol and acetic acid, the dicarbonitrile product was cyclotetramerized, yielding tetra 5,12-dioxo-5,12-dihydroanthro[2,3-b][1,4]dithiine-porphyrazine dye (2H-Pz) **4a**. Using metal salt and quinoline, the dicarbonitrile molecule was also cyclotetramerized, yielding the matching tetra 5,12-dioxo-5,12-dihydroanthro[2,3-b][1,4]dithiine-porphyrazinato-metal II dye (M-Pz), M = Zn **4b**, Co **4c**, or Ni **4d**.

The number of carbon atoms in the prepared dye structure reflects the envisioned structures presented in Scheme 1. Additionally, the metal concentration of the produced porphyrazines (see experimental) is comparable to that anticipated for the dye’s compositions predicted. The metal concentration (see experimental) and molecular mass of the generated dyes also show that the cyclo-tetramerization and chelation reactions are effective [24].



**Scheme 1.** Synthetic reaction rout of di-carbonitrile derivative **3** and porphyrazines **4a–4d**.

### 2.1. Infrared Spectra

Prominent bands at 1624, 3332, 1686, and 2226  $\text{cm}^{-1}$  are ascribed to the C=C, NH, C=O, and CN groups throughout the IR spectral information of component **3** (Figure 1). The stretching vibration of the C=N bond is related to the wide peak provided in the infrared investigation of product **4a** at 1522  $\text{cm}^{-1}$ . The absorption band of the C=N oscillation by Zn-porphyrazine dye **4b**, Co-porphyrazine dye **4c**, and Ni-porphyrazine dye **4d** at 1508, 1512, and 1516  $\text{cm}^{-1}$  (see experimental) is roughly 6–14  $\text{cm}^{-1}$  lower than that of the porphyrazine derivative **4a**, which depicts the engagement of a nitrogen atom of azomethine moiety with metallic salt ions in combinations. Additionally, a large peak appears at 3362  $\text{cm}^{-1}$ , which is explained by the oscillation of the N-H link stretching in the component **4a**. Since this oscillation of the N-H link is not found in that observed for dyes **4b–4d**, the NH unit is included in chelation process (Figure 2).

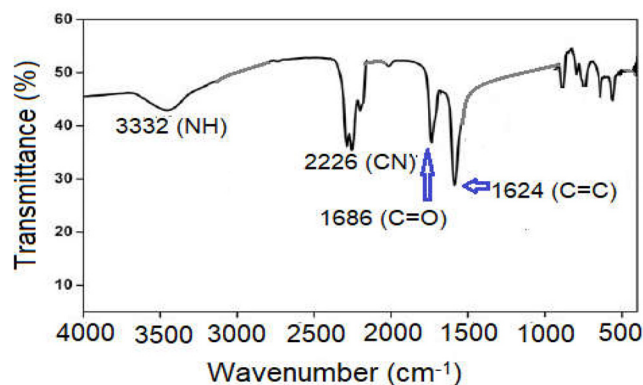


**Figure 1.** FT-IR spectra of dicarbonitrile **3**.

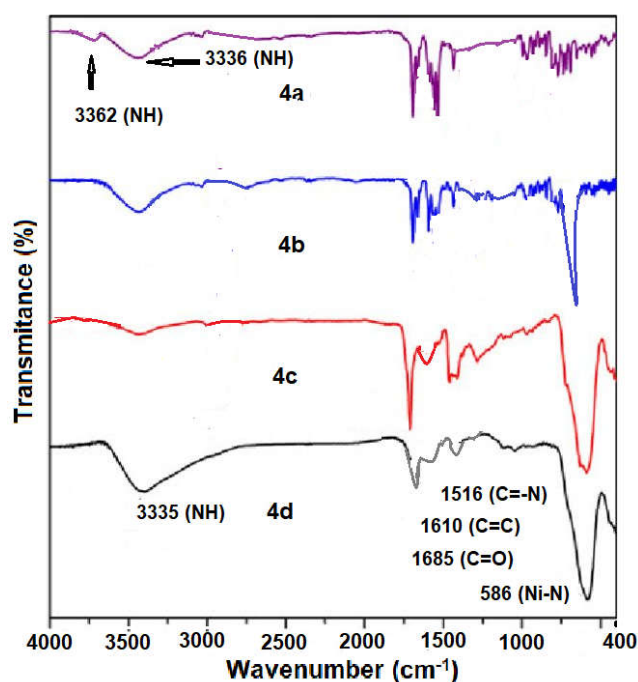


Figure 2. FT-IR spectra of porphyrazines 4a–4d.

## 2.2. Measurements of NMR and Molecular Mass

According to the structure of compound 3, the  $^1\text{H-NMR}$  spectrum shows a band at 6.28–6.85 ppm able to assign anthraquinone ring and benzene ring. Bands at 2.46 and 1.8 ppm belonging to  $\text{CH}_3$  and  $\text{NH}$  moieties are shown (Figure 3). The  $^{13}\text{C-NMR}$  spectrum identified bands at 24.4, 117.3, 123.5, 124.5, 127.7, 128.4, 128.8, 130.1, 138.0, and 187.1 ppm corresponding to  $\text{CH}_3$ ,  $\text{CN}$ ,  $\text{C=C}$  (thiin ring),  $\text{C=C}$  (anthraquinone ring, benzene ring), and  $\text{C=O}$ , respectively (Figure 4). The assigned formulation is compatible with the elemental analytical results of new product 3 (see experimental, Scheme 1).

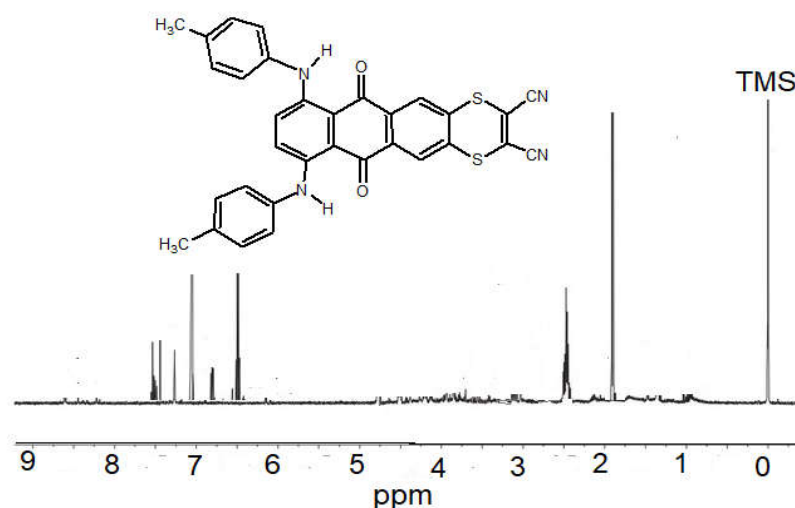
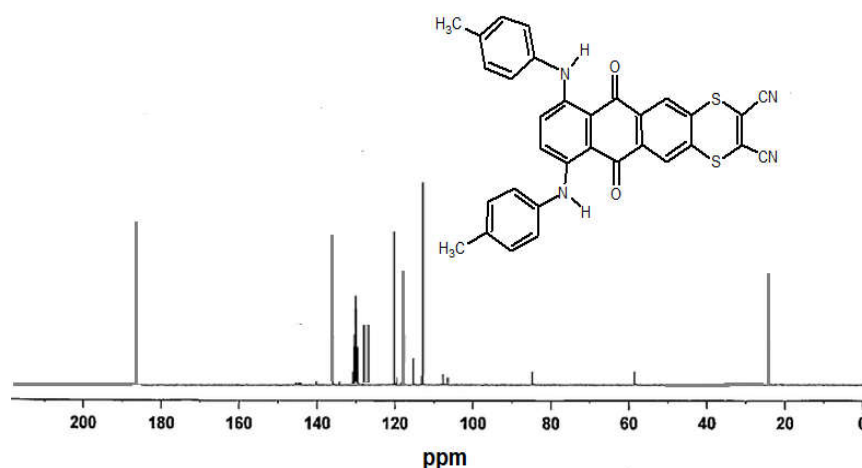
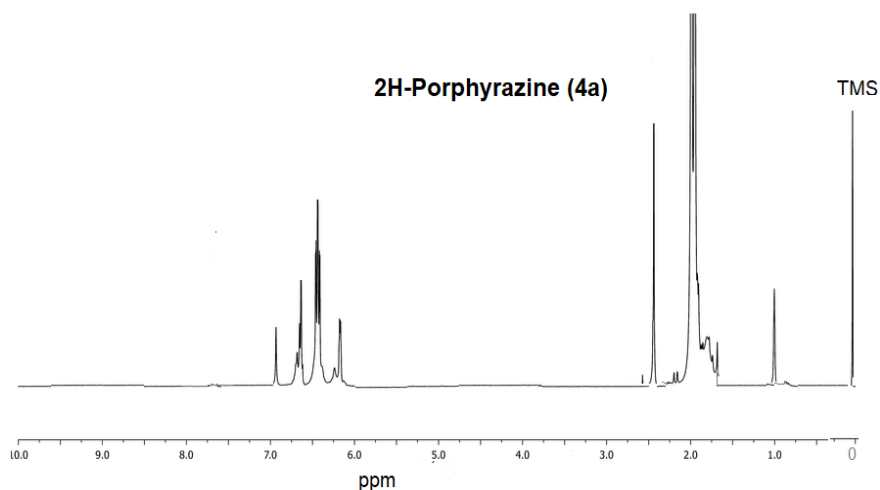


Figure 3.  $^1\text{H-NMR}$  spectra of dicarbonitrile 3.



**Figure 4.**  $^{13}\text{C}$ -NMR spectra of dicarbonitril **3**.

$^1\text{H}$ -NMR spectrum of **4a** (Figure 5) show two signals at 1.95 ppm (tolyl-NH) and 0.94 ppm (pyrrole moiety-NH) related to NH protons demonstrating the construction of a tetra-dentate ligand with an unsymmetrical structure. The  $^{13}\text{C}$ -NMR spectra of product **4a** (Figure 6) revealed a minor peak at 108.8 ppm, which can be attributed to the C=N group, and large bands at 24.8, 119.6, 138.6, 121.8, 134.9, 130.8, 137.0, 160.4, and 188.7 ppm, confirming the porphyrazine's structure. The  $^1\text{H}$ -NMR spectrum of **4b** (Figure 7) shows a signal at 1.95 ppm attributed to tolyl-NH. The absence of a signal in the spectra of **4b** related to the pyrrole moiety-NH ensures metal bonding with the pyrrole moiety-N. Figure 8 shows the  $^{13}\text{C}$ -NMR spectra of product **4b**, which indicated a minor band at 108.8 ppm that could be assigned to the CN group, as well as big bands at 23.8, 120.6, 137.2, 122.6, 135.2, 130.3, 137.26, 162.4, and 188.6 ppm that confirmed the structure of metal-porphyrazine. The compound **4c** is paramagnetic. The absence of a signal in the nmr spectrum of **4d** related to the pyrrole moiety-NH ensures metal bonding with the pyrrole moiety-N (Figure 9).  $^{13}\text{C}$ NMR spectrum of Ni-Porphyrazine complex **4d** (Figure 10) is in contestant with its expected structure.



**Figure 5.**  $^1\text{H}$ -NMR spectra of porphyrazine dye **4a**.

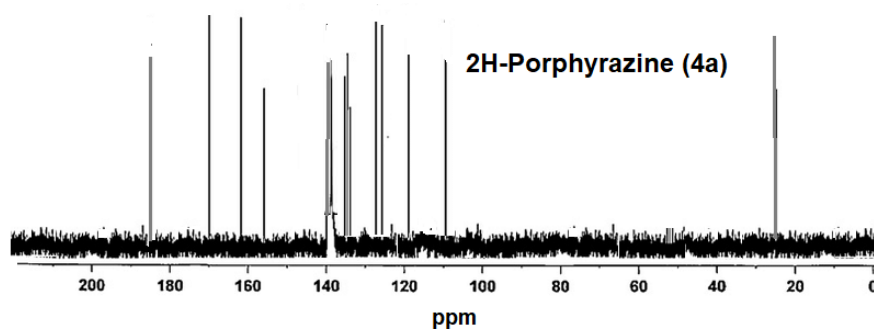


Figure 6.  $^{13}\text{C}$ -NMR spectra of porphyrazine dye 4a.

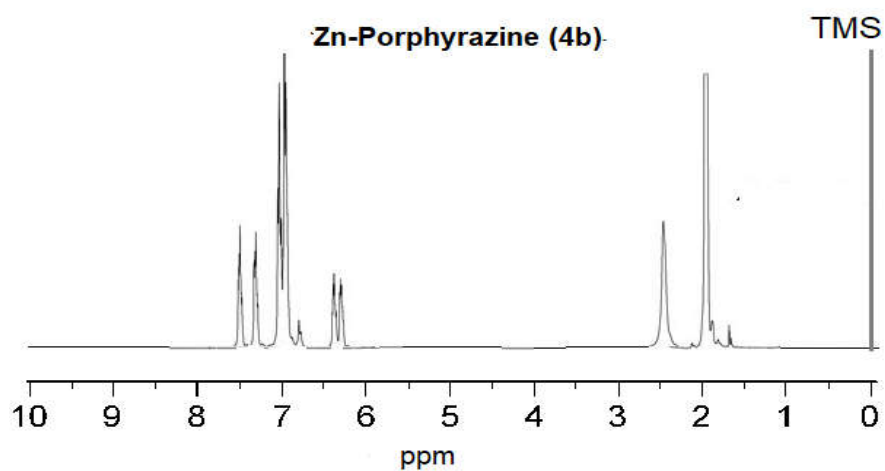


Figure 7.  $^1\text{H}$ -NMR spectra of porphyrazine dye 4b.

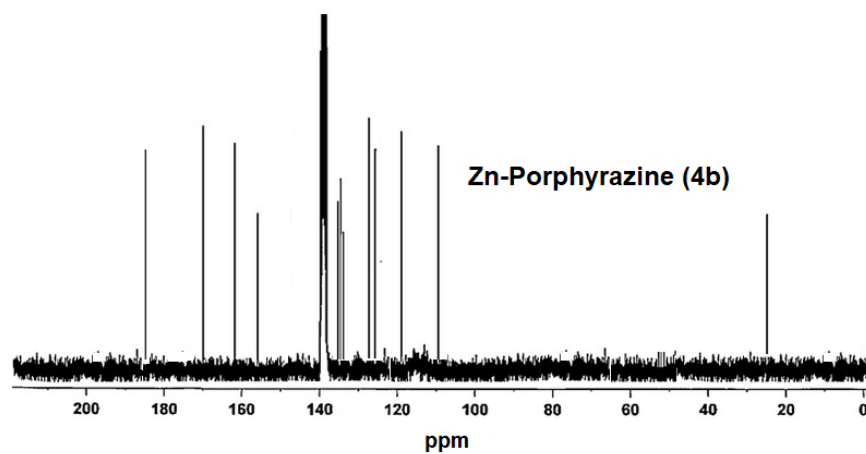


Figure 8.  $^{13}\text{C}$ -NMR spectra of porphyrazine dye 4b.

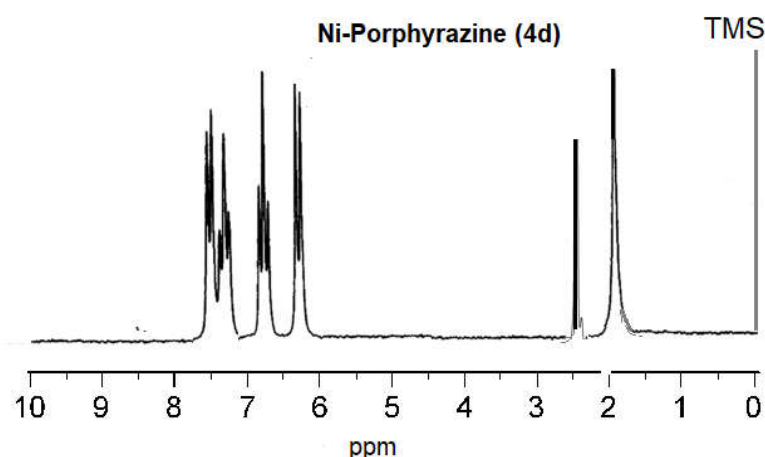


Figure 9.  $^1\text{H-NMR}$  spectra of porphyrzine dye **4d**.

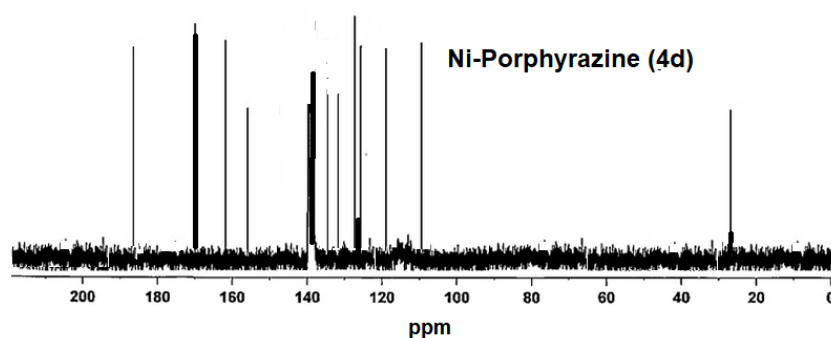
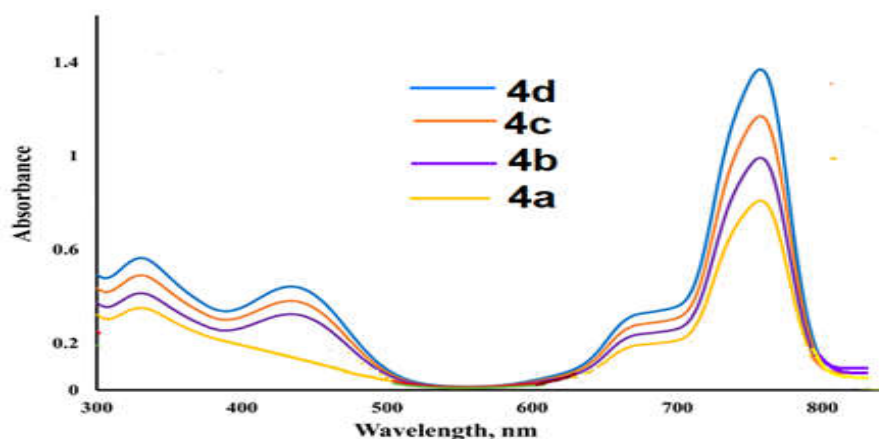


Figure 10.  $^{13}\text{C-NMR}$  spectra of porphyrzine dye **4d**.

### 2.3. Ultraviolet-Visible Spectra

A significant Soret band at 338 nm may be shown in ultraviolet-visible spectra of **4a** (Figure 11). The energy gap of both the high filled orbital and the low empty orbital enables the  $\pi\text{-}\pi^*$  shifts in compound **4a** that are illustrated at 663 and 752 nm. These bands closely resemble the characteristic bands mentioned in the literature [25]. In the characteristic spectroscopic analysis of the metallic contained combinations, **4b–d** in ethanol, the  $n\text{-}\pi^*$  and/or  $d\text{-}\pi^*$  transformations in the fused pyrrolo (1,4-dithiin) ring structure are conspicuous at larger B-peak (broad bands about 337 nm and narrow peaks at 446 nm) [26,27]. There are two distinct powerful fewer-energy Q-peaks (about 668 and 762 nm) that are highly developed. The transformation from **1s** to **4d** is commonly linked to the shoulder band [28]. At shorter wavelengths, interaction of the metal atom with binding modes leads to flip transformations, according to early theoretical studies [29,30]. All metal (1,4-dithiin)porphyrzines have peaks in the region of 436–445 nm beneath the Q-band. These states are caused by ligand metal exchange coupling and d-d excitations. The visible spectra of several metal (1,4-dithiin)porphyrzines varied by a small amount.





**Figure 11.** Ultraviolet-visible spectra of the porphyrazines **4a–4d**.

Transformation of charge from the metallic atom to the binder has been postulated to influence both the Q and B bands [31]. Metal complexes' absorption bands clearly extend beyond 800 nm. As a function, these dyes could be beneficial in applications requiring near-infrared absorption, such as optical information storage and safety photocopying. Both of the Soret and Q peaks could be understood using the Gouterman four orbital approach, which emerged from  $\pi-\pi^*$  transitions [32–34]. When compared to Co and Ni dyes, the transitions in Zinc dye are broader and moved toward longer wavelengths. The weaker signal at the reduced (elevated) part of the Q zone corresponds to the lowest charge carrier transformation for each dye. For Zn dye, it appears at 2.23 eV (663 nm), whereas for metal free and metal dyes, it occurs at 1.80–2.08 eV (665–672 nm). These energies represent the compounds' lowest limitations. As a result, the HOMO-LUMO separation of Co and Ni dyes is 0.25 eV fewer than that appeared in Zn dyes. This really is good for sunlight optical absorption since it closes the distance to the solitary cell's optimal (about 1.1–1.4 eV) [35]. The optical band ( $E_g$ ) was calculated from the last band edge at the highest frequency in UV-VIS absorption spectra (Figure 9). The last edge wavelength is at 800 nm and the  $E_g$  was calculated using the equation,  $E_g = 1240/\lambda = 1240/800 = 1.55$ . In all dyes, it primarily affects the nitrogen atoms of the chromophore, as well as the carbon atoms and anthra unit-accepting moieties. This verifies previous observations that such LUMO in Zn chromic dye is primarily located in the chromic dye center as just a  $\pi^*$ -orbital [36,37]. While the HOMO and LUMO of Zn dyes are situated in the same portion of the structure, notably the porphyrin circle and to a lesser degree the recipient group, there is a large spatial difference of the pair in Co and Ni dyes. The LUMO is part of the acceptor moiety, while the HOMO is part of the donor moiety, with some of them intersecting largely inside the chromophore. When electron-hole pairs in Zn-dye is separated spatially during solar irradiation, the recombination rate is reduced and the output current is increased.

### 3. Materials and Methods

#### 3.1. Characterization

All chemicals and solvents were purchased from commercial suppliers and used without purification. N,N-Dimethylformamide (anhydrous, 99.8%), Ethyl alcohol (96.0–97.2%), 1-Pentanol ( $\geq 99\%$ ), Quinoline (98%), Petroleum ether (AR, bp 40–60 °C), Acetone ( $\geq 99.5\%$ ), Lithium metal (99%), Zinc chloride ( $\geq 98\%$ ), Cobalt(II) chloride (97%), and Nickel(II) chloride (98%) were purchased from Sigma-Aldrich (St. Louis, MO, USA). 1,4-Bis(p-tolylamino)-6,7-dichloroanthraquinone {Merck}, and Di (sodiothio) maleonitrile {TCI (Shanghai) Development Co., Ltd., Shanghai, China} were used. Melting points (uncorrected) were determined in open capillaries on the Electrothermal melting point apparatus (Electrothermal Engineering Ltd., Rochford, UK). Spectral measurements were taken with Shimadzu 8101 M Fourier-transform infrared spectrometer. The spectrometer Uni-cam UV-Vis was used to obtain ultraviolet spectra. Utilizing tetramethyl silane as standard procedures, a



Varian VXR 400S NMR instrument operated at 400 MHz ( $^1\text{H}$ -NMR) and 100 MHz ( $^{13}\text{C}$ -NMR) was used, and NMR spectra were recorded in deuterio-chloroform. The metal content was determined using a Perkin Elmer Analyzer 300, AAS spectrometer. The elemental assessments were obtained utilizing PerkinElmer 2400 CHN. For monitoring the progress of a reaction, thin layer chromatography (TLC) was performed on pre-coated Merck (Darmstadt, Germany) silica gel 60F-254 plates using petroleum ether/acetone (10:5 *v/v*) as solvent system.

### 3.2. Synthesis of Dicarbonitrile Derivative **3**

1,4-Bis(*p*-tolylamino)-6,7-dichloroanthraquinone (0.01 mol) **1** and (0.01 mol) di (sodio-thio) maleonitrile **2** were heated at 80 °C for 8 h in the existence of dimethylformamide (50 mL). The product became brown at the finish of the reaction course period. It was filtered while heated, then deposited by an iced water, rinsed several times with water, left to dry, and crystallized from ethyl alcohol. A total of 88% product (yellowish brown crystallites); MP: 186 °C. Infrared spectra IR (KBr):  $\text{cm}^{-1}$ , 1624 (C=C), 1686 (C=O), 3332 (NH) and 2226 (CN);  $^1\text{H}$ -NMR ( $\text{CDCl}_3$ ): 1.8 ppm (aromatic C-NH), 2.46 ppm (CH<sub>3</sub>), 6.28–7.60 ppm (aromatic H).  $^{13}\text{C}$ -NMR ( $\text{CDCl}_3$ ): 24.4, 117.3, 119.0, 127.7, 128.4, 130.1, 138.0, and 187.10 ppm. Analysis Calculated for  $\text{C}_{32}\text{H}_{20}\text{N}_4\text{O}_2\text{S}_2$  (Mol. Wt.: 556.66) requires: C (69.04%), H (3.62%), N (10.06%). Found: C (69.13%), H (3.68%), N (10.11%).

### 3.3. Synthesis of the Dye Porphyrazine Derivative (2H-Pz) **4a**

A refluxing solution of **3** (0.5 mmol) in pentanol (100 mL) was mixed with lithium metal (20 mg, 2.8 mmol). The solution was heated for 16 h at reflux. After cooling, it was filtered while still hot, precipitated by an iced water, rinsed many times with  $\text{H}_2\text{O}$ , dried, and purified to crystals from ethanol. A total of 90% yield (brown crystallites). MP: 212 °C. IR [KBr]:  $\text{cm}^{-1}$ , 1522 (C=N), 1614 (C=C), 1690 (C=O), 3362 (NH), 3336 (NH). UV-Vis  $\lambda_{\text{max}}(\text{CH}_2\text{Cl}_2)/\text{nm}$ : 338, 663, 752.  $^1\text{H}$ -NMR ( $\text{CDCl}_3$ )  $\delta$  = 6.36–6.97 ppm (aromatic H), 0.94, 1.95 ppm (s, NH), 2.49 ppm (CH<sub>3</sub>).  $^{13}\text{C}$ -NMR spectrum revealed a small band at 24.8, 108.8 ppm able to assign CH<sub>3</sub> and C=N groups. Big bands at 119.6, 138.6, 121.8, 134.9, 130.8, 137.0 160.4, and 188.7 ppm. Analytical calculated for the expected porphyrazine  $\text{C}_{128}\text{H}_{84}\text{N}_{16}\text{O}_8\text{S}_8$ , Mol. Wt.: 2230.66, requires: C (68.92%), H (3.80%), and N (11.50%). Found: C (68.97%), H (3.86%), and N (10.11%).

### 3.4. Synthesis of the Dye Porphyrazinato-Metal II Derivatives (M-Pz) **4b–4d**

The appropriate metal complex was formed by heating the dinitrile monomer **3** (0.5 mmol) in quinoline (100 mL) at 200 °C for 16 h with 0.75 mmol of metallic salt (Zinc chloride, Cobalt chloride, or Nickel chloride). After the material was dissolved in acetone, the mis metal was recovered and extracted from the solution. It was purified while still heated, deposited with crushed ice, rinsed many times with distilled water, left to dry, and crystallized from ethyl alcohol. Vacuum drying was performed overnight on the product.

**4b**: 93% yield (deep brown crystals), MP: 208 °C. IR (KBr):  $\text{cm}^{-1}$ , 1508, (C=N), 3330 (NH), 1611 (C=C), 1686 (C=O). UV-Vis  $\lambda_{\text{max}}(\text{CH}_2\text{Cl}_2)/\text{nm}$ : 342, 452 (shoulder), 672 and 765.  $^1\text{H}$ -NMR ( $\text{CDCl}_3$ )  $\delta$  = 6.32–7.54 ppm (aromatic H), 1.98 ppm (s, NH), 2.44 ppm (CH<sub>3</sub>).  $^{13}\text{C}$ -NMR spectrum revealed a small band at 108.8 ppm able to assign C=N group and big bands at 23.8, 120.6, 137.2, 122.6, 135.2, 130.3, 137.26, 162.4, and 188.6 ppm. Analysis calculated for the expected porphyrazine  $\text{C}_{128}\text{H}_{82}\text{N}_{16}\text{O}_8\text{S}_8\text{Zn}$  (Mol. Wt.: 2294.03) requires: C (67.02%), H (3.60%), N (9.77%), and Zn (2.85%). Found: C (67.11%), H (3.67%), N (9.82%), and Zn (2.87%).

**4c**: 89% yield (Dark-green crystals), MP: 205 °C. IR [KBr]:  $\text{cm}^{-1}$ , 1512, (C=N), 3326 (NH), 1607 (C=C), 1688 (C=O). UV-Vis  $\lambda_{\text{max}}(\text{CH}_2\text{Cl}_2)/\text{nm}$ : 337, 446 (shoulder), 668 and 762. Analysis calculated for the expected porphyrazine  $\text{C}_{128}\text{H}_{82}\text{N}_{16}\text{O}_8\text{S}_8\text{Co}$  (Mol. Wt.: 2287.58) requires: C (67.21%), H (3.61%), N (9.80%), and Co (2.58%). Found: C (67.28%), H (3.66%), N (9.87%), and Co (2.65%).

**4d**: 91% yield (brown crystals), MP: 203 °C. IR [KBr]:  $\text{cm}^{-1}$ , 1516, (C=N), 3335 (NH), 1610 (C=C), 1685 (C=O). UV-Vis  $\lambda_{\text{max}}$  ( $\text{CH}_2\text{Cl}_2$ )/nm: 334, 440 (shoulder), 665 and 759.  $^1\text{H-NMR}$  ( $\text{CDCl}_3$ )  $\delta$  = 6.30–7.57 ppm (aromatic H), 1.95 ppm (s, NH), 2.34 ppm ( $\text{CH}_3$ ).  $^{13}\text{C-NMR}$  spectrum revealed a small band at 108.8 ppm able to assign C=N group and big bands at 24.0, 120.3, 138.2, 121.4, 134.3, 131.3, 138.0, 161.7, and 185.9 ppm. Analysis calculated for the expected porphyrazine  $\text{C}_{128}\text{H}_{82}\text{N}_{16}\text{O}_8\text{S}_8\text{Ni}$  (Mol. Wt.: 2287.34) requires: C (67.21%), H (3.61%), N (9.80%), and Ni (2.57%). Found: C (67.28%), H (3.68%), N (9.88%), and Ni (2.66%).

#### 4. Conclusions

Tetra free metal- and [1,4]dithiine-porphyrazinato-metal II dye derivatives light sensitizers were produced. The metal concentration and molecular mass of the generated dyes show that the cyclo-tetramerization and chelation reactions are effective. The prepared substituted porphyrazines reveal high absorption in the UV–VIS region, which could be of potential value as a building block for novel electronic and optical materials as well as a sensor for technology. The presence of electron-donating amine groups reduced the optical band gap of organometallic sensitizers with a “push–pull” structure by about 1.55 eV.

**Author Contributions:** Conceptualization, H.H.A.-R., O.A.A.A., M.A. and E.F.; methodology; software; validation; formal analysis; investigation; resources; data curation; writing—original draft preparation; H.H.A.-R., O.A.A.A., M.A. and E.F. writing—review and editing; visualization; supervision; project administration; funding acquisition. All authors have read and agreed to the published version of the manuscript.

**Funding:** Taif University Researchers Supporting Project number (TURSP-2020/220), Taif University, Taif, Saudi Arabia.

**Data Availability Statement:** The data presented in this study are available on request from the corresponding author.

**Acknowledgments:** The authors would like to thank the Deanship of Scientific Research at Taif University for funding this work through Taif University Researchers Supporting Project number (TURSP-2020/220), Taif University, Taif, Saudi Arabia.

**Conflicts of Interest:** The authors declare no conflict of interest.

#### References

1. Sudarsan, V. *Functional Materials, 8—Optical Materials: Fundamentals and Applications*; Banerjee, S., Tyagi, A.K., Eds.; Elsevier: Amsterdam, The Netherlands, 2012; pp. 285–322.
2. Jorg, K.; Subramanian, L.R.; Michael, H.J. Synthesis of silicon tetrapyrzino-porphyrazines. *J. Porphyr. Phthalocyanines* **2000**, *4*, 498–504.
3. Turubanova, V.D.; Mishchenko, T.A.; Balalaeva, I.V.; Efimova, I.; Peskova, N.N.; Klapshina, L.G.; Lermontova, S.A.; Bachert, C.; Krysko, O.; Vedunova, M.V.; et al. Novel porphyrazine-based photodynamic anti-cancer therapy induces immunogenic cell death. *Sci. Rep.* **2021**, *11*, 7205. [[CrossRef](#)] [[PubMed](#)]
4. Tang, J.; Chen, L.; Sun, J.; Lv, K.; Deng, K. Synthesis and properties of iron(II) tetra(1,4-dithiin)porphyrazine bearing peripheral long-chain alkyl group of active end-bromine. *Inorg. Chem. Commun.* **2010**, *13*, 236–239. [[CrossRef](#)]
5. Deng, K.; Huang, F.; Wang, D.; Peng, Z.; Zhou, Y. A Novel Catalyst Iron(II) Tetra(1,4-dithiin)porphyrazine for Oxygenating Degradation of Organic Pollutants in Aqueous Solutions. *Chem. Lett.* **2004**, *33*, 34–35. [[CrossRef](#)]
6. Faust, R.; Weber, C.J. Three-step synthesis and absorption and emission properties of peripherally peralkynylated tetrapyrzino-porphyrazines. *Org. Chem.* **1999**, *64*, 2571–2573. [[CrossRef](#)]
7. Yang, C.; Sun, J.; Deng, K.; Wang, D. Synthesis and photocatalytic properties of iron(II)tetramethyl-tetra(1,4-dithiin)porphyrazine. *Catal. Commun.* **2008**, *9*, 321–326. [[CrossRef](#)]
8. Abdel-Razik, H.H.; Abbo, M.; Almahy, H.A.; Kenawy, E. Synthesis, characterization and spectroscopic investigation of novel tetra-(1,4-dithiin)porphyrazine network polymers derived from dithianone monomer. *Macromol. Indian J. (MMAIJ)* **2013**, *9*, 45–50.
9. Jin, J.; Yang, C.; Hang, B.Z.; Deng, K. Selective oxidation of amines using  $\text{O}_2$  catalyzed by cobalt thioporphyrazine under visible light. *J. Catal.* **2018**, *361*, 33–39. [[CrossRef](#)]
10. Zhou, Q.; Xu, S.; Yang, C.; Zhang, B.; Li, Z.; Deng, K. Modulation of peripheral substituents of cobalt thioporphyrazines and their photocatalytic activity. *Appl. Catal. B Environ.* **2016**, *192*, 108–115. [[CrossRef](#)]

11. Lu, G.; Chu, F.; Huang, X.; Li, Y.; Liang, K.; Wang, G. Recent advances in Metal-Organic Frameworks-based materials for photocatalytic selective oxidation. *Coord. Chem. Rev.* **2022**, *450*, 214240. [[CrossRef](#)]
12. Zervaki, G.E.; Tsaka, V.; Vatikioti, A.; Georgakaki, I.; Nikolaou, V.; Sharma, G.D.; Coutsolelos, A.G. A triazine di(carboxy)porphyrin dyad versus a triazine di(carboxy)porphyrin triad for sensitizers in DSSCs. *Dalton Trans.* **2015**, *44*, 13550–13564. [[CrossRef](#)] [[PubMed](#)]
13. Zhao, L.; Wagner, P.; Salm, H.; Clarke, T.M.; Gordon, K.C.; Mori, S.; Mozer, A.J. Dichromophoric Zinc Porphyrins: Filling the Absorption Gap between the Soret and Q Bands. *J. Phys. Chem. C* **2015**, *119*, 5350–5363. [[CrossRef](#)]
14. Tuncer, S.; Koca, A.; Gül, A.; Avciata, U. Synthesis, characterization, electrochemistry and spectroelectrochemistry of novel soluble porphyrazines bearing unsaturated functional groups. *Dyes Pigm.* **2011**, *92*, 610–618. [[CrossRef](#)]
15. Yella, A.; Lee, H.W.; Tsao, H.N.; Yi, C.; Chandiran, A.K.; Nazeeruddin, M.K.; Diau, E.W.G.; Yeh, C.Y.; Zakeeruddin, S.M.; Gratzel, M. Porphyrin-Sensitized Solar Cells with Cobalt (II/III)-Based Redox Electrolyte Exceed 12% Efficiency. *Science* **2011**, *334*, 629–634. [[CrossRef](#)]
16. Bessho, T.; Zakeeruddin, S.M.; Yeh, C.Y.; Diau, E.W.G.; Gratzel, M. Highly Efficient Mesoscopic Dye-Sensitized Solar Cells Based on Donor-Acceptor-Substituted Porphyrins. *Angew. Chem.* **2010**, *122*, 6796–6799. [[CrossRef](#)]
17. Wu, S.L.; Lu, H.P.; Yu, H.T.; Chuang, S.H.; Chiu, C.L.; Lee, C.W.; Diau, E.W.G.; Yeh, C.Y. Design and Characterization of Porphyrin Sensitizers with a Push-Pull Framework for Highly Efficient Dye-Sensitized Solar Cells. *Energy Environ. Sci.* **2010**, *3*, 949–955. [[CrossRef](#)]
18. Keskin, B.; Denктаş, C.; Altındal, A.; Avciata, U.; Gül, A. Synthesis of Ni(II) porphyrazine peripherally octa-substituted with the 4-tert-butylbenzylthio moiety and electronic properties of the Al/Ni(II)Pz/p-Si Schottky barrier diode. *Polyhedron* **2012**, *38*, 121–125. [[CrossRef](#)]
19. Stuzhin, P.A.; Bauer, E.M.; Ercolani, C. Syntheses and properties of tetrakis(thiadiazole)porphyrazine and its magnesium and copper derivatives. *Inorg. Chem.* **1998**, *37*, 1533–1539. [[CrossRef](#)]
20. Ekaterina, N.T.; Hamdoush, M.; Eroshin, A.V.; Ryzhov, I.V.; Zhabanov, Y.A.; Stuzhin, P.A. Tetra(1,2,5-thiadiazolo) porphyrazines. 10. Synthesis, spectral characterization and DFT study of complexes with yttrium(III) and lutetium(III). *Polyhedron* **2021**, *193*, 114877.
21. Stuzhin, P.; Ivanova, S.; Hamdoush, M.; Kirakosyan, G.; Kiselev, A.; Popov, A.; Sliznev, V.; Ercolani, C. Tetrakis(1,2,5-thiadiazolo)porphyrazines. 9. Synthesis and spectral and theoretical studies of the lithium(i) complex and its unusual behaviour in aprotic solvents in the presence of acids. *Dalton Trans.* **2019**, *48*, 14049–14061. [[CrossRef](#)]
22. Zhabanov, Y.A.; Ryzhov, I.V.; Kuzmin, I.A.; Eroshin, A.V.; Stuzhin, P.A. DFT Study of Molecular and Electronic Structure of Y, La and Lu Complexes with Porphyrazine and Tetrakis(1,2,5-thiadiazole)porphyrazine. *Molecules* **2021**, *26*, 113. [[CrossRef](#)]
23. Yahya, M.; Bouziani, A.; Ocaк, C.; Seferođlu, Z.; Sillanpää, M. Organic/metal-organic photosensitizers for dye-sensitized solar cells (DSSC): Recent developments, new trends, and future perceptions. *Dyes Pigm.* **2021**, *192*, 109227. [[CrossRef](#)]
24. Kim, J.; Jaung, J.Y.; Ahn, H. Tetrapyrzazinoindoloporphyrazine Langmuir-Blodgett films. *Macromol. Res.* **2008**, *16*, 367. [[CrossRef](#)]
25. Jaung, J.Y.; Matsuoka, M.; Fukunishi, K. Syntheses and characterization of push-pull tetrapyrzazino[2,3-b] indoloporphyrazines. *Synthesis* **1998**, *1998*, 1347–1351. [[CrossRef](#)]
26. Puigdollers, J.; Voz, C.; Fonrodona, M.; Cheylan, S.; Stella, M.; Andreu, J.; Vetter, M.; Alcubilla, R. Copper phthalocyanine thin-film transistors with polymeric gate dielectric. *J. Non-Cryst. Solids* **2006**, *352*, 1778. [[CrossRef](#)]
27. Wizel, S.; Margel, S.; Gedanken, A.; Rojas, T.C.; Fernandez, A.; Prozorov, R. The preparation of metal-polymer composite materials using ultrasound radiation: Part II. Differences in physical properties of cobalt-polymer and iron-polymer. *J. Mater. Res.* **1999**, *14*, 3913. [[CrossRef](#)]
28. Bruder, I.; Schöneboom, J.; Dinnebier, R.; Ojala, A.; Schäfer, S.; Sens, R.; Erk, P.; Weis, J. What determines the performance of metal phthalocyanines (MPc, M = Zn, Cu, Ni, Fe) in organic heterojunction solar cells? A combined experimental and theoretical investigation. *Org. Electron.* **2010**, *11*, 377–387. [[CrossRef](#)]
29. Cory, M.G.; Zerner, M.C. Metal-ligand exchange coupling in transition-metal complexes. *Chem. Rev.* **1991**, *91*, 813–822. [[CrossRef](#)]
30. Chen, Q.; Gu, D.; Gan, F. Ellipsometric spectra of cobalt phthalocyanine films. *Phys. B* **1995**, *212*, 189. [[CrossRef](#)]
31. Gouterman, M. Study of the Effects of Substitution on the Absorption Spectra of Porphyrin. *J. Chem. Phys.* **1959**, *30*, 1139–1161. [[CrossRef](#)]
32. Gouterman, M. Spectra of Porphyrins. *J. Mol. Spectrosc.* **1961**, *6*, 138–163. [[CrossRef](#)]
33. Baerends, E.; Ricciardi, G. A DFT/TDDFT Interpretation of the Ground and Excited States of Porphyrin and Porphyrazine Complexes. *Coord. Chem. Rev.* **2002**, *230*, 5–7. [[CrossRef](#)]
34. Cook, P.L.; Yang, W.; Liu, X.; García-Lastra, J.M.; Rubio, A.; Himpsel, F.J. Unoccupied States in Cu and Zn Octaethyl-Porphyrin and Phthalocyanine. *J. Chem. Phys.* **2011**, *134*, 204707. [[CrossRef](#)] [[PubMed](#)]
35. Katoh, R.; Furube, A. Electron injection efficiency in dye-sensitized solar cells. *J. Photochem. Photobiol. C Photochem. Rev.* **2014**, *20*, 1–16. [[CrossRef](#)]
36. García-Lastra, J.M.; Cook, P.L.; Himpsel, F.J.; Rubio, A. Communication: Systematic shifts of the lowest unoccupied molecular orbital peak in X-ray absorption for a series of 3d metal porphyrins. *J. Chem. Phys.* **2010**, *133*, 151103. [[CrossRef](#)] [[PubMed](#)]
37. Zulkifli, M.; Said, N.; Aziz, B.; Shujahadeen, B.; Hisham, S.; Shah, S.; Bakar, A.; Abidin, Z.; Tajuddin, H.; Sulaiman, L.; et al. Electrochemical Characteristics of Phthaloyl Chitosan Based Gel Polymer Electrolyte for Dye Sensitized Solar Cell Application. *Int. J. Electrochem. Sci.* **2020**, *15*, 7434–7447. [[CrossRef](#)]